Implementations of control laws for motion camouflage in a pursuit-evasion system

Carmeliza Navasca, Ani Asatryan,Vatche Attarian,Yuan R. Huang, Kevin K. Leung
Abhijeet Joshi, Vlad Voroninski, Meghdi Aboulian, Krystle McBride

***Abstract*— Motion camouflage is a sly technique found in nature and employed by bats and hoverflies. We analyze the pursuit-evader system by introducing strategies for both players for capturing its prey and escaping its predator. Analytical bounds for feedback laws and sufficient conditions for initial cost and intial conditions are found to guarantee either capture or evasion in finite time. We also have numerical implementation satisfying the inequalities. Moreover, the steering laws are implemented in a testbed to check feasibility in a real environment.**

Introduction

Motion camouflage is a sly technique that allows a pursuer to approach a prey while appearing to remain stationary from the viewpoint of the prey. To accomplish this, the pursuer follows a way such that it always lies on the line that connects the pursuer and fixed point. If the pursuer is approaching the prey, the only visual signal to the pursuers approach is its threatening. The prey identifies no movement away from the direction of the fixed point. The fixed point could be an existing sight in the framework or the initial position of the pursuer. There is some clue of motion camouflage observed in nature; for instance, it has been suggested that bats use motion camouflage to minimize the time to capture of a moving prey. In [9], [1], the experimental data suggests motion camouflage interactions between hoverflies.

In this work, we extend the work of Justh and Krishnaprasad [4] on steering laws for motion camouflage. An earlier study of the mathematics of motion camoulfage by Glendinning [2]. We analyze the interaction of both the pursuer and evader when the strategies are present. In [4], feedback laws are derived from a cost function based on the ratio of change of the baseline vector corresponding on the positions of the pursuer and evader. In addition, analytical studies show bounds on the gain to guarantee capture at some time. Here we analyze the bounds on the gains for both the strategies of the players in the pursuit and evasion cases. Moreover, we also have numerical simulations to verify the analytical bounds as well as testbed simulations for the steering laws to demonstrate its feasibility in a real environment.

I. Modeling Equations

The equations of motion for the players are the following [4],[8], and the references therein:

$$\begin{aligned}\dot{r}_p &= x_p,\\ \dot{x}_p &= y_p u_p,\\ \dot{y}_p &= -x_p u_p.\end{aligned} \tag{1}$$

and

$$\begin{aligned}\dot{r}_e &= \nu x_e,\\ \dot{x}_e &= \nu y_e u_e,\\ \dot{y}_e &= -\nu x_e u_e.\end{aligned} \tag{2}$$

where r_p and r_e are the position of the pursuer and evader, respectively. The corresponding unit tangent vectors are x_p and x_e while the unit normal vectors are denoted y_p and y_e. In addition, the controls u_p and u_e are the curvatures of r_p and r_e, respectively. The systems of equations (1) and (2) are so-called Frenet-Serret equations. The derivation of these equations can be found in [5].

In the work of Justh and Krishnaprasad [4], the control law u_p is a motion camouflage feedback which forces the *pursuer to be in the same constant bearing as the evader*.

Definition 1.1: Motion camouflage with respect to the point at infinity is

$$r = \lambda \bar{r}$$

where

$$r = r_p - r_e,$$

$\bar{r}$ is a unit vector, and $\lambda \in \mathbb{R}$.

The cost function associated with the motion camouflage is

$$\Gamma(t) = \frac{\frac{d}{dt}|r|}{|\frac{dr}{dt}|}, \tag{3}$$

Vatche Attarian and Krystle McBride are with Harvey Mudd College, Claremont, USA

Meghdi Aboulian, Ani Asatryan, Yuan R. Huang, Kevin K. Leung, Abhijeet Joshi, Vlad Voroninski are with the Dept. of Mathematics, University of California, Los Angeles, USA

Carmeliza Navasca is with Centre National de la Recherche Scientifique (CNRS), ETIS Lab - École Nationale Supérieure de l' Électronique et de ses Applications (ENSEA), 6 avenue du Ponceau, 95014 Cergy-Pontoise, FRANCE, navasca@ensea.fr

which is the ratio of the rate of change of the baseline vector r and the absolute rate of change of the baseline vector. Moreover, because $\frac{d}{dt}|r| = \frac{r}{|r|} \cdot \dot{r}$ we have that

$$\Gamma(t) = \frac{r}{|r|} \cdot \frac{\dot{r}}{|\dot{r}|} \tag{4}$$

Then, by differentiating (4) w.r.t. the trajectories (1) and (2) and using

$$\begin{aligned} \dot{r}^{\perp} &= y_p - \nu y_e, \\ \dot{\dot{r}} &= y_p u_p - \nu^2 y_e u_e, \\ \dot{r}^{\perp} \cdot y_p &= 1 - \nu(x_p \cdot x_e), \\ &\text{and} \\ \dot{r}^{\perp} \cdot y_e &= (x_p \cdot x_e) - \nu \end{aligned}$$

we have

$$\begin{aligned} \dot{\Gamma} &= \frac{|\dot{r}|}{|r|}\left[\frac{1}{|\dot{r}|^2}\left(\frac{r}{|r|}\cdot\dot{r}^{\perp}\right)^2\right] \qquad (5) \\ &+ \frac{|\dot{r}|}{|r|}\left[\frac{1}{|\dot{r}|^2}\left(\frac{r}{|r|}\cdot\dot{r}^{\perp}\right)\right]\left(1-\nu\left(x_p\cdot x_e\right)\right)u_p \\ &+ \frac{|\dot{r}|}{|r|}\left[\frac{1}{|\dot{r}|^2}\left(\frac{r}{|r|}\cdot\dot{r}^{\perp}\right)\right]\left(\nu-\left(x_p\cdot x_e\right)\right)\nu^2 u_e \end{aligned}$$

A. Control feedback for evasion

In this section, we present a motion camouflage strategy for the evader for an evader-evadee system. In [4], the authors studied the pursuer's motion camouflage strategy for a pursuer-pursee system analytically and numerically. In both of these cases, only the evader and pursuer use strategies for capture or evasion of its oblivious adversaries. So this is not truly game. For a pursuit-evasion game, we must include strategies of both players. Thus, this motivates us to study first motion camouflage strategy for the evader; i.e. the evader conceals its motion from the evadee while maintaining or elongating the baseline vector $|r|$.

The motion camouflage strategy is

$$u_e = \beta\left(\frac{r}{|r|}\cdot\dot{r}^{\perp}\right) \tag{6}$$

where $\beta > 0$. Note that the strategy for the pursuer has a negative gain $-\mu$ for sufficiently large μ. In our evader-evadee system, we assume that u_p is bounded and continuous on some interval.

Theorem 1.1: Consider the systems (1) and(2) with the cost function (4) and control law (6) along with the following assumptions:

- $0 < \nu < 1$
- u_p is continuous and bounded on some interval
- $\Gamma_0 < 1$
- $|r(0)| > 0$.

Then for $\epsilon, \epsilon_0 > 0$ where $\epsilon = \min(\epsilon_0, 1-\Gamma_0^2)$ there exists $t^* \in [0,T]$ such that $\Gamma(t^*) > 1+\epsilon$; i.e. motion camouflage is attainable in finite time.

Proof: We wish to show that at some time t^* for which $\Gamma(t^*) \geq 1-\epsilon$. In order to find a bound, we solve the equation from (5), (6),

$$\dot{\Gamma} \geq c_0(1-\Gamma^2) + c_1\sqrt{1-\Gamma^2}$$

where

$$c_0 = \frac{1-\nu}{|r|} + \frac{\beta(\nu-1)\nu^2}{1+\nu} \tag{7}$$

and

$$c_1 = \frac{\min(u_p)(\nu-1)}{1+\nu}.$$

Then let $1-\Gamma^2 > \epsilon$ where $\epsilon = \min(\epsilon_0, 1-\Gamma_0^2)$ and $\epsilon_0 > 0$ is *how close we choose* Γ *is to* 1. It follows that

$$\dot{\Gamma} \geq c_2(1-\Gamma^2)$$

where $c_2 = c_0 - \frac{c_1}{\sqrt{\epsilon}}$. Thus, solving the equation above,

$$\Gamma(t) \geq \tanh(\tanh^{-1}\Gamma_0 - c_2 t). \tag{8}$$

It follows that whenever $c_2 = \frac{\left(\frac{1}{2}\ln\left(\frac{2-\epsilon}{\epsilon}\right) - \tanh^{-1}\Gamma_0\right)}{t}$ we have that $\Gamma(t) \geq 1-\epsilon$. Equation (7) implies that

$$\beta \leq \frac{c_0(1+\nu)}{(\nu-1)\nu^2} + \frac{1+\nu}{\nu^2|r|} \quad \forall\ |r| > r_0 \tag{9}$$

where $r_0 > 0$ and $r_0 < |r(0)|$. The bound in (8) is valid $\forall\ |r| > r_0 \Leftrightarrow \forall\ t \leq \frac{|r(0)|-r_0}{1+\nu}$. It follows that $c_2 \geq \frac{(1+\nu)\left(\frac{1}{2}\ln\left(\frac{2-\epsilon}{\epsilon}\right) - \tanh^{-1}\Gamma_0\right)}{|r(0)|-r_0}$. Thus, if $T = \frac{|r(0)|-r_0}{1+\nu}$, then motion camouflage is attained at some time $t^* \in [0,T]$. ■

Remark. Our proof is in the spirit of Justh and Krishnaprasad [4].

B. Pursuit-Evasion Games

In this section, we study the interaction of the players in a pursuit-evasion game, that is, when both control feedback strategies are present. Let the strategies be

$$\begin{aligned} u_p &= -\mu\left(\frac{r}{|r|}\cdot\dot{r}^{\perp}\right) \qquad (10) \\ &\text{and} \\ u_e &= \beta\left(\frac{r}{|r|}\cdot\dot{r}^{\perp}\right) \qquad (11) \end{aligned}$$

where $\beta, \mu \geq 0$. In the following theorem, we find some sufficient conditions for the pursuer to capture the evader while maintaining motion camouflage.

Theorem 1.2: Consider the systems (1) and(2) with the cost function (4) and control laws, (10) and (11), along with the following assumptions:

- $0 < \nu < 1$

- $\Gamma_0 < 1$
- $|r(0)| > 0$.

Then for $\epsilon, \epsilon_0 > 0$ where $\epsilon = \min(\epsilon_0, 1-\Gamma_0^2)$ there exists $\tilde{c}_2$ such that $\dot{\Gamma} \leq -\tilde{c}_2(1-\Gamma^2)$ and $t^* \in [0, T]$ such that $\Gamma(t^*) < -1+\epsilon$. Moreover, the gains from both strategies satisfy the inequality $\mu \geq \beta$.

Proof: We show that there exist t^* such that $\Gamma(t^*) > -1+\epsilon$. Here $\epsilon = \min(\epsilon_0, 1-\Gamma_0^2)$ and $\epsilon_0 > 0$ is how close we choose Γ is to -1. Note that when $\Gamma = -1$ we have the baseline vector r in pure contraction regime from (3). From (5), we have

$$\begin{aligned}\dot{\Gamma} \leq \; & -(1-\Gamma^2)\left[\frac{\mu}{|\dot{r}|}(1-\nu(x_p \cdot x_e)) - \frac{|\dot{r}|}{|r|}\right] \\ & + \sqrt{1-\Gamma^2}\left|\frac{\beta(\nu-(x_p \cdot x_e))}{|\dot{r}|}\left(\frac{r}{|r|}\cdot \dot{r}^{\perp}\right)\right|.\end{aligned}$$

By using the bounds $1-\nu \leq |\dot{r}| \leq 1+\nu$,

$$\begin{aligned}\dot{\Gamma} \leq \; & -(1-\Gamma^2)\left[\frac{\mu(1-\nu)}{1+\nu} - \frac{1+\nu}{|r|}\right] \\ & + \sqrt{1-\Gamma^2}\left[\frac{\beta\nu^2(1+\nu)^2}{(1-v)^2}\right].\end{aligned}$$

Now let

$$\tilde{c}_0 = \left[\frac{\mu(1-\nu)}{1+\nu} - \frac{1+\nu}{|r|}\right] \quad (12)$$

and

$$\tilde{c}_1 = \left[\frac{\beta\nu^2(1+\nu)^2}{(1-v)^2}\right] \quad (13)$$

so that

$$\dot{\Gamma} \leq -\tilde{c}_0(1-\Gamma^2) + \tilde{c}_1\sqrt{1-\Gamma^2}.$$

For $(1-\Gamma^2) > \epsilon$, the equation above reduces to

$$\dot{\Gamma} \leq -\tilde{c}_2(1-\Gamma^2) \quad (14)$$

where

$$\tilde{c_2} = \tilde{c}_0 - \frac{\tilde{c}_1}{\sqrt{\epsilon}} \geq 0. \quad (15)$$

From (12) and (13), we have

$$\mu \geq \left(\frac{1+\nu}{1-\nu}\right)\left(\frac{1+\nu}{r_0} + \tilde{c}_0\right) \quad (16)$$

and

$$\beta \geq \frac{(1-\nu)^2}{\nu^2(1+\nu)^2}\tilde{c}_1 \quad (17)$$

for some $\tilde{c}_0 > 0$ and $\tilde{c}_1 > 0$ satisfying (15) and some $\tilde{r}_0 > 0$. In fact, we have

$$\mu \geq \left(\frac{1+\nu}{1-\nu}\right)\left(\frac{1+\nu}{\tilde{r}_0} + \frac{\tilde{c}_1}{\sqrt{\epsilon}}\right) \geq \beta\frac{\nu^2(1+v)^2}{\sqrt{\epsilon}(1-\nu)^2}$$

which implies that $\mu \geq \beta$. Solving the equation (14), we get $\Gamma(t) \leq \tanh(\tanh\Gamma_0 - \tilde{c}_2 t)$. This equation is valid for $t \in [0, T]$ where $T = \frac{|r(0)|-\tilde{r}_0}{1+\nu}$. Thus, $\Gamma(t^*) \leq -1+\epsilon$ for some time $t^* \in [0, T]$ if $\tilde{c}_0$ and $\tilde{c}_1$ in (15) are chosen sufficiently large so that $\tilde{c}_2 \geq \frac{(1+\nu)\left(-\frac{1}{2}\ln\left(\frac{2-\epsilon}{\epsilon}\right)+\tanh^{-1}\Gamma_0\right)}{|r(0)|-r_0}$. ■

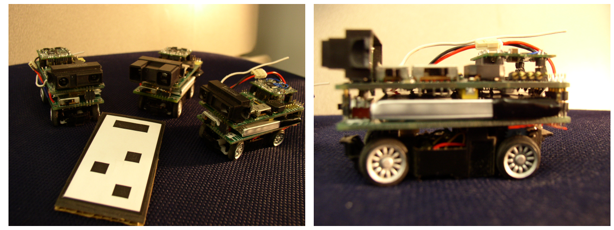

Fig. 1. Vehicles at UCLA Applied Math Lab

In consequence, we have the following result for evasion.

Theorem 1.3: Consider the systems (1) and(2) with the cost function (4) and control laws, (10) and (11), along with the following assumptions:

- $0 < \nu < 1$
- $\Gamma_0 < 1$
- $|r(0)| > 0$.

Then for $\epsilon, \epsilon_0 > 0$ where $\epsilon = \min(\epsilon_0, 1-\Gamma_0^2)$ there exists $\hat{c}_2$ such that $\dot{\Gamma} \geq \hat{c}_2(1-\Gamma^2)$ and $t^* \in [0, T]$ such that $\Gamma(t^*) > 1-\epsilon$. Moreover, the gains from both strategies satisfy the inequality $\beta > \mu$.

Proof: See the proof of Theorem 1.2. Here β and μ must satisfy the inequalities

$$\beta \leq \left(\hat{c}_0 - \frac{1-\nu}{\hat{r}_0}\right)\left(\frac{1+\nu}{(\nu-1)\nu^2}\right) \quad (18)$$

and

$$\mu \leq \hat{c}_1\left(\frac{1+\nu}{1-\nu}\right) \quad (19)$$

for some $\hat{c}_0, \hat{c_1}, \hat{r}_0 > 0$. In addition, for sufficiently large $\hat{r}_0$, one can show $\beta > \mu$. ■

II. Testbed Adaptation

In order to demonstrate its feasibility in a real environment, we implement one of the steering laws introduced in [4] onto the UCLA Applied Math Lab micro-car testbed [3]. The testbed is comprised of two major components, a tracking system and car-like vehicles (Fig. 1). The tracking system provides real-time location and heading information, which is sent to the vehicles wirelessly at 30Hz. The vehicle is an ordinary rear-wheel-drive vehicle. A tiny servo integrated into the vehicle's chassis allows 51 (left 25, center, and right 25) degrees of steering freedom. Table.I shows some physical parameters of the vehicles. See the paper [7] for more details on the construction of the testbed.

Dimension(L × W × H)	$(7 \times 3.5 \times 7)$ cm
Weight	68 g
Minimum Turning Radius	$15 \sim 20$ cm
Steering Range	$-25° \sim 25°$
Speed Range	$30 \sim 90$ cm/s

TABLE I

PHYSICAL PARAMETERS OF THE VEHICLES

A. Control Law Adaptation

We implement the MCPG curvature law (10)

$$u_p = -\mu \left(\frac{r}{|r|} \cdot \dot{r}^{\perp} \right)$$

which does not require the adversary vehicle's steering program. Thus the vehicles without sensor in micro-car testbed are used in our implementation. Recall that u_p is the curvature control of the pursuer and μ is assumed to be sufficiently large so that the evader's steering program can be neglected.

Currently, the testbed overhead tracking system only provides the position and the heading angle, the angle between the vehicle's direction of motion and x-axis of the testbed. By equation

$$\dot{r}^{\perp} = y_p - \nu y_e,$$

the MCPG steering law becomes

$$u_p = -\mu \left(\cos\theta_p - \nu \cos\theta_e \right)$$

where θ_p is the angle between r and y_p, θ_e is the angle between r and y_e. Then, the angles θ_p and θ_e can be easily calculated from the vehicles' headings. To map the curvature control u_p into the vehicle's desired steering angle, we model our vehicle as a simple car as in [6]. The steering angle ϕ_p of a simple car and its corresponding turning radius (ρ) satisfies the following relation:

$$\rho = \frac{L}{\tan\phi_p} \tag{20}$$

where L represents the distance between the vehicle's front and rear wheels. For the vehicles in the testbed $L = 4$cm. Then the steering angle of a pursuer can be calculated as

$$\begin{aligned} \phi_p &= \tan^{-1}(L/\rho) \\ &= \tan^{-1}(L u_p) \\ &= \tan^{-1}\left[L\mu \left(\nu\cos\theta_e - \cos\theta_p \right) \right] \end{aligned} \tag{21}$$

Recall that the vehicle's wheels have limited turning range; see Table.I. Thus, the constrained steering angle is defined as

$$\phi_p^c = \begin{cases} -25° & \text{if } \phi_p \le -25° \\ \phi_p & \text{if } -25° < \phi_p < 25° \\ 25° & \text{if } \phi_p \ge 25°. \end{cases} \tag{22}$$

Note that ϕ_p, as specified in (21), steers a vehicle towards its target while maintaining motion camouflage. Then, symmetrically $-\phi_p$ steers away its target while maintaining motion camouflage. Thus

$$\phi_e = -\tan^{-1}\left[L\beta \left(\nu\cos\theta_p - \cos\theta_e \right) \right] \tag{23}$$

Note that we would also constrain ϕ_e in the same fashion as in (22). In addition, the MCPG steering law also assumes that the pursuer moves at unit speed, while the evader moves at a constant speed $\nu < 1$. Moreover, to maintain coherence with the players' speed, all the parameters with length dimension are scaled according to the actual vehicular speed. For instance, if the vehicle actually moves at 40 cm/s, L would be scaled down to 0.1.

III. EXPERIMENTAL RESULTS

A. Testbed Simulations

We performed several experiments with two vehicles for three cases: (a) pursuer-pursuee, (b) evader-evadee, and (c) pursuer-evader, where the pursuee and evadee are neutral agents that follow some arbitrary controls. The parameters used in the simulations are: $L = 0.067, \mu = 15, \beta = 15$, and $\nu = 0.75$. For the cases a and b, with $\nu < 1$ the simulation always results in the capture of the evader or pursuee. From the vehicular trajectory plots (Figs. 2, 3, and 4), we can clearly see that the baseline vector r is able to maintain its initial orientation with only minor deviations. We attribute these deviations to the sundial mechanical conditions of the vehicles and noise in the vehicular heading estimate, which has a maximum error of approximately $\pm 2.5°$.

B. Computer Simulations

The numerical simulations were utilized to study the behavior of pursuer-pursuee, evader-evadee, and pursuer-evader systems with individual agents under the control laws (10), (11), or a constant steering control. The codes are run in Matlab using the forth-order Runge-Kutta method for solving (1) and (2). In all numerical examples, the evader speed is $\nu = .9$ while the pursuer moves at a unit speed. Figure 5 illustrates the behavior of a pursuer-pursuee system where the steering law of the pursuer is the motion camouflage proportional guidance (MCPG) with μ satisfying the inequalities provided (and similar to those in (9)) in [4]. The pursuee trajectory is determined by the control law $u_e = 0$, corresponding to straight line motion, and $u_e = c$ where c is positive constant, corresponding to circular motion. Similarly, we implement the evader-evadee system in Fig. 6 with the evader's control law u_e given by (11) with $\beta = 13.2$ satisfying the bounds (9). The cost function $\Gamma(t)$ is plotted for the trajectories in Figs. 5 and 6. In Fig. 5(left), $\Gamma(t)$ tends to -1 from an initial

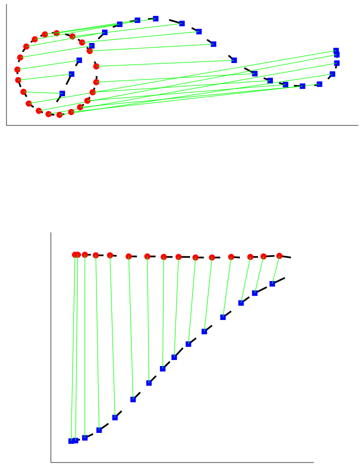

Fig. 2. The trajectories of a pursuer-pursuee pair. The round dots represent the pursuee, as the square dots represent the pursuer. Top: the pursuee traverses a circle; Bottom: the pursuee traverses a straight line.

value $\Gamma(t_0) > -1$; motion camouflage is sustained in the pursuit. The cost function $\Gamma(t)$ corresponding to the evasion illustrated in the former figure is plotted and oscillates in the range [0,1] until it stabilizes about 1. Since $\Gamma(t) = 1$ corresponds to the lengthening of $|r|$ at time t, we can deduce that choosing control u_e preserves motion camoulfage while conferring an evader the additional advantage of increasing the distance between it and a potential pursuer.

In Figs. 7 and 8, we simulate several games in which both pursuer and evader control laws, (10) and (11) respectively, are implemented simultaneously. In Figure 7, the trajectories of the agents are presented for various initial conditions and values of the parameters μ and β satisfying (16), (17), (18), and (19). We observe that the values of these parameters, as well as initial conditions such as $\Gamma(0)$ and $|r|$, determine the success of pursuer and evader control strategies. Figure 8 contains the plots of the cost function $\Gamma(t)$ versus time for the games presented in Figure 7. As one can see, the value of Γ tends to approach either 1 or -1, corresponding to the instances where pursuit or evasion prevail respectively.

IV. Acknowledgements

Voroninski and Joshi are supported by NSF RTG grant DMS-0601395. We are grateful for having access to the UCLA Applied Math Lab which is supported by ARO grant W911NF-5-1-0112, ONR grant N000140610059, and MURI grant 50363-MA-MUR.

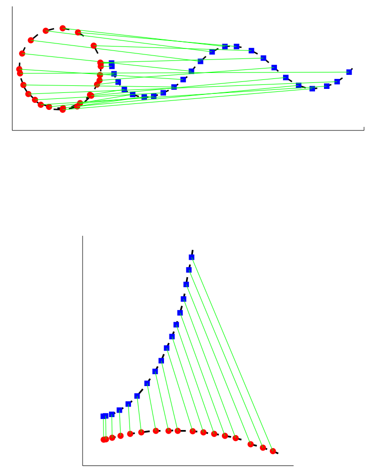

Fig. 3. The trajectories of a evader-evadee pair. The round dots represent the evadee, as the square dots represent the evader. Top: the evadee traverses a circle; Bottom: the evadee traverses a line.

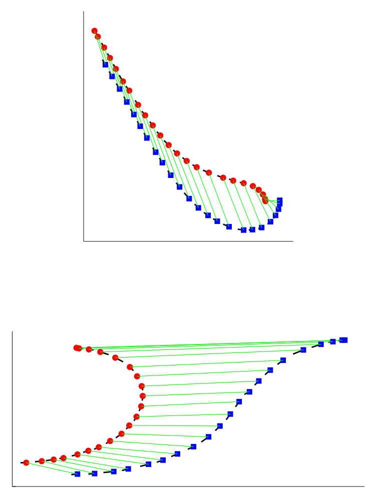

Fig. 4. The above figures show the trajectories of a pursuer-evader pair. The round dots represent the evader, as the square dots represent the pursuer. Top: the pursuer and the evader are positioned close-by while facing opposite directions initially; Bottom: the pursuer and the evader are positioned relatively far away while facing each other initially.

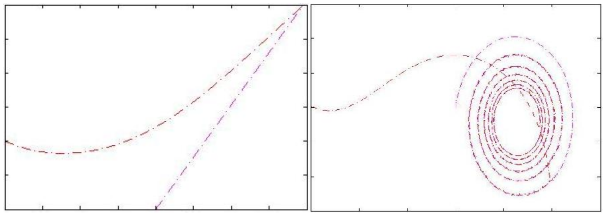

Fig. 5. Trajectories for pursuer-pursuee model with $\mu = 500$ in MCPG law and the pursuee's steering law $u_e = 0$ (left) and $u_e = c$, constant (right)

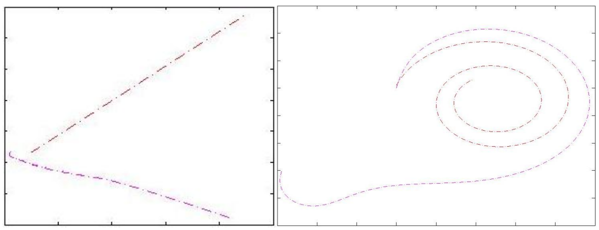

Fig. 6. Trajectories for evader-evadee model with the evadee's steering law $u_p = 0$ (left) and $u_p = c$, constant (right)

REFERENCES

[1] T.S. Collett and M.F. Land, "Visual control of flight behaviour in the hoverfly, Syritta pipiens," J. Comp. Physiol., vol. 99, pp. 1-66, 1975.

[2] P. Glendinning, "The mathematics of motion camouflage," Proc. Roy. Soc. Lond. B, Vol. 271, No. 1538, pp. 477-481, 2004.

[3] C. H. Hsieh, Y. L. Chuang, Y. Huang, K. K. Leung, A. L. Bertozzi, and E. Frazzoli, "An economical micro-car testbed for validation of cooperative control strategies," *Proc. American Contr. Conf.*, Minneapolis, MN, 2006.

[4] E. W. Justh and P. S. Krishnaprasad, "Steering laws for motion camouflage," Preprint.

[5] V. Jurdjevic, Geometric Control Theory, Cambridge University Press, Cambridge, UK, 1997.

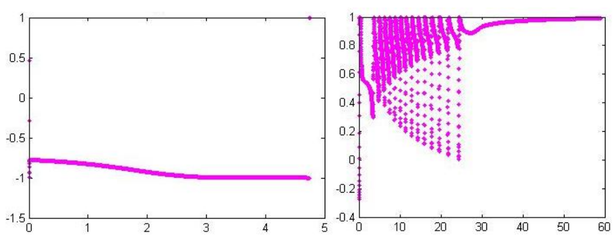

Fig. 7. Cost function $\Gamma(t)$

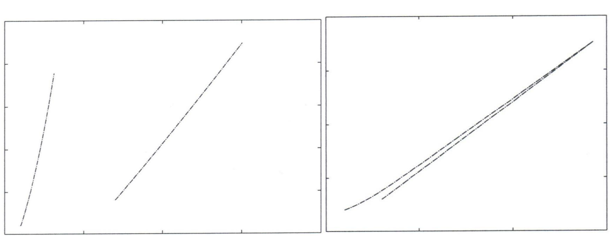

Fig. 8. Pursuer-evader model: $\mu = 500$, $\beta = 900$ (left) and $\mu = 500$, $\beta = 13.2$ (right)

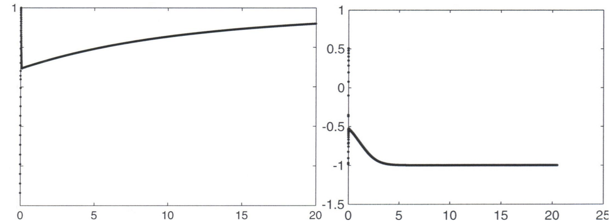

Fig. 9. Cost function $\Gamma(t)$ for Fig. 4: evasion (left) and capture (right)

[6] S. M. LaValle, "Planning Algorithms", Cambridge University Press, 2006

[7] K. K. Leung, C. H. Hsieh, Y. R. Huang, A. Joshi, V. Voroninski, and A. Bertozzi, " A second generation microvehicle testbed for cooperative control and sensing strategies," submitted to ACC 2006.

[8] D. S. Morgan and Ira B. Schwartz, "Dynamic coordinated control laws in multiple agent models, " Physics Letters A 340 (2005) 121-131.

[9] M.V. Srinivasan and M. Davey, "Strategies for active camouflage of motion," Proc. Roy. Soc. Lond. B, Vol. 259, No. 1354, pp. 19-25, 1995.